

# NUMERICAL MODELLING AND COMPUTATION OF FLUID PRESSURE TRANSIENTS WITH AIR ENTRAINMENT IN PUMPING INSTALLATIONS

T. S. LEE

*Mechanical Engineering Department, Faculty of Engineering, National University of Singapore, 10 Kent Ridge Crescent, Singapore 0511*

## SUMMARY

In pumping installations such as sewage pumping stations, where gas content and air entrainment exist, the computation of fluid pressure transients in pipelines becomes grossly inaccurate when a constant wave speed is assumed. An accurate numerical model with gas release and absorption has been developed in this paper and used to compute the fluid pressure transients in the pumping mains of selected pumping installations. Free and dissolved gases in the transported fluid and cavitation at vapour pressure are also modelled. When compared with the gas-free case, computations show that entrained, entrapped or released gases amplify the positive pressure peak, increase surge damping and produce asymmetric pressure surges. While the upsurge with air entrainment in the pipelines was considerably amplified, the downsurge was only marginally reduced. The computed results show good agreement with the data available.

**KEY WORDS** Air entrainment Pressure surges Wave speed Pumping installations

## INTRODUCTION

In numerous pipeline flow systems the fluid medium may be entrained and saturated with one or more gases in which stabilized gas nuclei necessary for cavitation inception are known to exist. Under transient conditions, owing to extreme pressure fluctuations, the flow regime can change from a single-phase medium to a two-phase medium as the dissolved gas is released during low-pressure periods—a phenomenon termed gas release or gaseous cavitation. Since the gas evolution rate is higher than the solution rate, as the pressure oscillates with time about the gas saturation pressure, rectified diffusion occurs, resulting in a net gain of free gas during each cycle. Consequently, the wave speed for the mixture is reduced owing to the added compressibility of the gas, which in turn may give rise to significant dispersion of the pressure wave. In contrast with gaseous cavitation, if the local fluid pressure falls to its vapour pressure, sudden growth of the nuclei, now containing vapour and free gas, will occur—a process which is manifested in flashing behind a negative pressure wave or, in the more severe situation, in column separation. Whereas the latter process of vaporous cavitation takes place in a few microseconds, gaseous cavitation is a much slower process, being of the order of one to several seconds.

In sewage pumping stations, for example, air entrainment into the system can occur owing to (i) the falling jets of sewage from the comminutors into the sump near the operating pump bellmouths, (ii) the attached vortex formation arising from the operation of the pumps or (iii) the adverse flow path towards the operating pumps. Flow in the pipelines will also contain free gas, although the volumetric proportion may be small. Trapped air pockets at the top of pipe

cross-sections at high points along the pipe profile can also be present owing to (i) the incomplete removal of air during commissioning and filling-up operation or (ii) progressive upward migration of pockets of air. Air may also be admitted into the pipeline owing to vortex action at an inadequately designed air vessel. Most sewage also contains dissolved gases in solution. Gas bubbles will be evolved from the liquid during the passage of low-pressure transients. When the liquid is subject to high transient pressures, the free gas will be compressed and some may be dissolved. The process is highly time- and pressure-dependent. The resultant pressure surges can thus be expected to be complex.

Whiteman and Pearsall<sup>1,2</sup> were the first to study the effects on pressure transients when air was entrained into the fluid of a pumping station. Pump shut-down tests were conducted with reflux valve closure on two sewage pumping stations with air entrained into the fluid. In general the first pressure peak with entrained air in the pipeline was found to be higher than that predicted by the constant wave speed water hammer theory. Previous investigations related to pipeline transients with air entrainment and gaseous evolution can be described according to the assumed flow regime and analytical model utilized. Two different types of air entrainment models have been proposed in the literature for predicting the above pressure transient behaviour, namely the concentrated vaporous cavity model<sup>3,4</sup> and the air release model.<sup>5-7</sup> The concentrated vaporous cavity model confines the vapour cavities to fixed computing sections and uses a constant wave speed for the fluid in reaches between the cavities. The air release model assumes the evolved and free gas to be distributed throughout the reaches, thereby requiring variable wave speeds which are dependent on gas content and local pressure.

It was evident from the earlier investigations mentioned above that by including gas release, reasonable predictions of initial pressure surge were obtained. However, with few exceptions, proper phasing and attenuation of subsequent predicted peaks remained in error. Little is known at this stage concerning the physical process of gaseous diffusion in a closed conduit subjected to unsteady flow; in part this is due to the random nature of bubble nucleation, coalescence and growth in turbulent flow fields. Much more research in this field is needed.

#### AIR ENTRAINMENT AND GAS RELEASE VARIABLE WAVE SPEED MODEL

Earlier investigations by Lee<sup>8</sup> showed that the presence of undissolved gas bubbles in a fluid greatly reduces the wave speed. The effect of free air on wave speed is more significant under low-pressure conditions, where its volume is greater than under high-pressure conditions. The variable wave speed model proposed here assumes the presence of free entrained air content  $\epsilon_0$  and dissolved gas content  $\epsilon_g$  in the liquid at atmospheric pressure. Assumptions were made that (i) the gas-liquid mixture is homogeneous, (ii) the free gas bubbles in the liquid follow a polytropic compression law with  $n = 1.2-1.3$  and (iii) the pressure within the air bubbles during the transient process is in equilibrium with the local fluid pressure. *When the computed local transient pressure falls below the fluid gas release pressure  $p_g$ , an instantaneous release of dissolved gas of  $\alpha_{gr}\epsilon_g$  is observed.* The local pressure remains constant and is equal to the vapour pressure. *When the computed transient pressure recovers to a value above the gas release pressure, the equivalent amount of gas redissolved into the liquid is observed to be  $\alpha_{gd}\epsilon_g$ .* Since the local pressure remains constant when the computed pressure is below the gas release pressure, the maximum air content has a limit and hence the wave speed also has a lower limit which is consistent with the data observed.

Consider a mass of liquid containing a fractional volume  $\epsilon$ , of gas in free bubble form. It can

be shown that the effective bulk modulus  $K_T$  of the gas-liquid mixture, including the pipe distensibility effect and pipe constraint condition  $c$ , is given by<sup>7,8</sup>

$$\frac{1}{K_T} = \frac{1}{K} + \frac{\varepsilon}{np} + \frac{cD}{eE}, \quad (1)$$

while the local wave speed  $a_i$  at an absolute pressure  $p_i$  and air fraction content  $\varepsilon_i$  is given by

$$a_i^k = \left[ \rho_w (1 - \varepsilon_i^k) \left( \frac{1}{K} + \frac{\varepsilon_i^k}{np_i^k} + \frac{cD}{eE} \right) \right]^{-1/2}. \quad (2)$$

For this model of variable wave speed the initial free air fraction  $\varepsilon_o$  and dissolved gas fraction  $\varepsilon_g$  at a reference absolute pressure  $p_o$  must be specified. The initial variable wave speed along a pipeline ( $i = 0, 1, \dots, N$ ) is then computed through the absolute pressure distribution along the pipeline from equation (2) at  $k = 0$  (steady state).

The transient computation of the fraction of air content along the pipeline depends on the local pressure and local air volume and is given by

$$\varepsilon_T^{k+1} = \left( \frac{p_i^k}{p_i^{k+1}} \right)^{1/n} \varepsilon_i^k \quad \text{and} \quad \varepsilon_o^{k+1} = \left( \frac{p_o}{p_i^{k+1}} \right)^{1/n} \varepsilon_o; \quad (3a)$$

for  $p_i^{k+1} \geq p_g$  and  $\varepsilon_T^{k+1} \leq \varepsilon_o^{k+1} + \alpha_{gr} \varepsilon_g$

$$\varepsilon_i^{k+1} = \varepsilon_T^{k+1}; \quad (3b)$$

for  $p_i^{k+1} \geq p_g$  and  $\varepsilon_T^{k+1} > \varepsilon_o^{k+1} + \alpha_{gr} \varepsilon_g$

$$\varepsilon_i^{k+1} = \left( \frac{p_i^k}{p_i^{k+1}} \right)^{1/n} (\varepsilon_i^k - \alpha_{ga} \varepsilon_g); \quad (3c)$$

for  $p_i^{k+1} < p_g$

$$\varepsilon_i^{k+1} = \left( \frac{p_i^k}{p_g} \right)^{1/n} (\varepsilon_i^k + \alpha_{gr} \varepsilon_g). \quad (3d)$$

The above air fraction content is then substituted into equation (2) to obtain the wave speed along the pipeline for the next time level computation. For water saturated at atmospheric pressure the gas release pressure head approaches that of the vapour pressure (i.e. 2.4 m water absolute). A typical free air content in sewage at atmospheric pressure is about 0.1%; the free gas content evolved at the gas release head is about 2.0% at atmospheric head. The fraction of gas absorption is  $\alpha_{ga} = 0.3$  and the fraction of gas release is  $\alpha_{gr} = 0.6$ .<sup>4,9,10</sup>

## METHOD OF CHARACTERISTICS WITH VARIABLE WAVE SPEED

The method of characteristics applied to the pressure transient problem with variable wave speed  $a_i$  as modelled above can be described<sup>7</sup> by the respective  $C^+$  and  $C^-$  characteristic equations

$$\frac{g}{a} \frac{dH}{dt} + \frac{dV}{dt} + \frac{g}{a} V \sin \alpha + \frac{f_i}{2D} V |V| = 0, \quad (4)$$

$$dx/dt = V + a \quad (5)$$

and

$$-\frac{g}{a} \frac{dH}{dt} + \frac{dV}{dt} + \frac{g}{a} V \sin \alpha + \frac{f_i}{2D} V|V| = 0, \tag{6}$$

$$dx/dt = V - a. \tag{7}$$

The loss factor  $f_i$  used in conjunction with the method of characteristics with air entrainment and gas release in a pipeline system is evaluated at the local point  $i$  using the characteristics of the flow at that point. The steady state overall loss factor at the operating point of a system can be determined from the pump characteristic curve and system curve.

With reference to the irregular  $t$ -grid and regular  $x$ -grid notation used in Figure 1,  $i$  denotes the regular  $x$ -mesh point value at location  $x = (i\Delta x)$  and  $k$  denotes the irregular time level corresponding to the time at  $t^k = \sum (\Delta t^k)$ . The value of the time step  $\Delta t_k$  at each time level is determined by the CFL criterion

$$\Delta t^k = \min[k_i \Delta x / (|V_i| + a_i)] \quad \text{for } i = 0, 1, \dots, N, \tag{8}$$

where  $k_i$  is a constant less than 1.0.

The characteristic equations specified by (4)–(7) can thus be approximated by the finite difference expressions

$$\frac{g}{a_R} \frac{H_i^{k+1} - H_R}{\Delta t^k} + \frac{V_i^{k+1} - V_R}{\Delta t^k} + \frac{g}{a_R} V_R \sin \alpha_i + \frac{f_{iR}}{2D} V_R |V_R| = 0, \tag{9}$$

$$\frac{x_i - x_R}{\Delta t^k} = V_R + a_R \tag{10}$$

and

$$-\frac{g}{a_S} \frac{H_i^{k+1} - H_S}{\Delta t^k} + \frac{V_i^{k+1} - V_S}{\Delta t^k} + \frac{g}{a_S} V_S \sin \alpha_i + \frac{f_{iS}}{2D} V_S |V_S| = 0, \tag{11}$$

$$\frac{x_i - x_S}{\Delta t^k} = V_S - a_S, \tag{12}$$

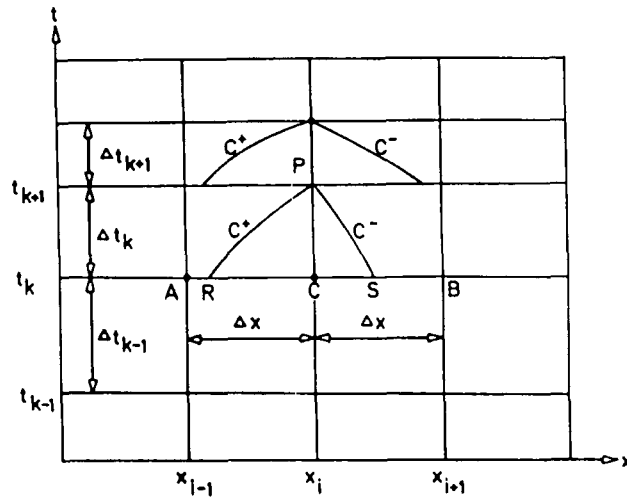


Figure 1. Computational grid for variable wave speed with variable time steps

where R is the point of interception of the  $C^+$  characteristic line on the  $x$ -axis between node points  $(i - 1)$  and  $i$  at the  $k$ th time level and S is the point of interception of the  $C^-$  characteristic line on the  $x$ -axis between node points  $i$  and  $i + 1$ . With conditions known at points  $i - 1$ ,  $i$  and  $i + 1$  at the  $k$ th time level, the conditions at R and S can be evaluated by a linear interpolation procedure. The conditions at R and S are then substituted into equations (9)–(12) and the solutions at the  $(k + 1)$ th time level at point  $i$  are obtained for  $i = 0, 1, \dots, N$ . A mesh size of  $N = 1000$  was used for the solutions presented in this work.

### BOUNDARY CONDITIONS

A common flow arrangement in water and sewage engineering consists of (i) a lower reservoir, (ii) a group of pumps with a check valve in each branch and (iii) a pipeline discharging into an upper reservoir (water tower, gravity conduit, aeration well, etc.). In order to safeguard the pipeline and its hydraulic components from over- and/or underpressurization, it is important to determine extreme pressure loads under transient conditions. Pump stoppage is an operational case which has to be investigated and which often gives rise to maximum and minimum pressures. The most severe case occurs when all the pumps in a station fail simultaneously owing to a power failure. In this case the flow in the pipeline rapidly diminishes to zero and then reverses. The pump also rapidly loses its forward rotation and reverses shortly after the reversal of the flow. As the pump speed increases in the reverse direction, it causes great resistance to the backflow, which produces high pressure in the discharge line near the pump. To prevent reverse flow through the pump, a check valve is usually fitted immediately after each pump. When the flow reverses, the check valve is activated and closed. A large pressure transient occurs in the pipeline when the flow reverses and the check valves of the pumps close rapidly.

The equivalent pump characteristics in the pumping station during pump stoppage and pump run-down can be described by the homologous relationship for  $n_p$  pumps as

$$H_e^{k+1} = A_1(N^{k+1})^2 + (A_2/n_p)(N^{k+1})Q_0^{k+1} + (A_3/n_p^2)(Q_0^{k+1})^2, \quad (13)$$

$$T_e^{k+1} = (B_1 n_p)(N^{k+1})^2 + B_2(N^{k+1})Q_0^{k+1} + (B_3/n_p)(Q_0^{k+1})^2, \quad (14)$$

$$\eta_e^{k+1} = C_1 + (C_2/n_p)(Q_0^{k+1}/N^{k+1}) + (C_3/n_p^2)(Q_0^{k+1}/N^{k+1})^2, \quad (15)$$

$$T_e = -I_e d\omega/dt, \quad (16)$$

where  $H_0^{k+1} = H_e^{k+1}$ ,  $I_e = n_p I$ ,  $\omega = 2\pi N$ ,  $Q$  is the flow rate,  $n_p$  is the number of pumps,  $A_1, A_2, A_3, B_1, B_2, B_3$  and  $C_1, C_2, C_3$  are single-pump constants and  $H_e, T_e$  and  $\eta_e$  are the equivalent pump head, torque and efficiency respectively. The efficiency of the equivalent pump during pump run-down is assumed to be equal to the efficiency of the corresponding single-pump run-down efficiency. Equation (13) is to be solved together with the  $C^-$  characteristic line described by equations (11) and (12) for a pump speed  $N^{k+1}$  determined from equations (14)–(16) by the procedures following Fox,<sup>7</sup> using the concept of an equivalent pump when there is more than one pump operating in a pumping station. The changes in pump speed during pump run-down for both normal and turbine modes are modelled. When reverse flow is encountered in the pump, the check valve is assumed closed. At this instant  $V_0^{k+1}$  is assumed to be zero for the  $C^-$  characteristic line at  $i = 0$  for all subsequent time levels. In the case where the check valve closure time is known, the flywheel or pumpset inertia can be sized such that the pump continues delivery for a period longer than the check valve closure time. This will ensure non-reversal of flow before the check valve is able to close. Downstream of each of the above profiles is assumed a constant head reservoir, i.e.  $H_N^{k+1} = \text{const.}$  for all time levels, and this is solved with the  $C^+$  characteristic line for  $V_N^{k+1}$  for each time level.

## RESULTS AND DISCUSSION

The effects of variable wave speed on pressure transients generated by simultaneous pump trip at pumping stations were studied using three pumping stations. Pumping station A (Figure 2) uses three parallel centrifugal pumps to supply  $0.73 \text{ m}^3 \text{ s}^{-1}$  of water to a tank  $21.5 \text{ m}$  above sump level through a  $0.7 \text{ m}$  diameter main of  $1243 \text{ m}$  length. Pumping station B (see Figure 5) uses two parallel centrifugal pumps to supply  $0.195 \text{ m}^3 \text{ s}^{-1}$  of water to a tank  $40 \text{ m}$  above the sump level through a  $0.5 \text{ m}$  diameter main of  $1550 \text{ m}$  length. Pumping station C (see Figure 8) uses three parallel centrifugal pumps to supply  $1.08 \text{ m}^3 \text{ s}^{-1}$  of water to a tank  $19.7 \text{ m}$  above the sump level through a  $0.985 \text{ m}$  diameter main of  $4720 \text{ m}$  length. The reflux valve downstream of the pumping station was assumed to close instantaneously when flow reverses at the pump.

Figures 3, 4 and 6, 7 show the effect of air entrainment and gas release in the variable wave speed model on the pressure transient for pumping stations A and B respectively in comparison with that using a constant wave speed model with no air content. The figures show that gas release and air entrainment increase the maximum pressure upsurge along the pipeline and reduce the magnitude of the negative pressure downsurge. The corresponding numerical experiments with pumping station C (Figures 9–11) using the variable wave speed model also show similar results. Three distinct pressure transient characteristics were observed from the above numerical experiments: (i) the first pressure peak is above that predicted by the constant wave speed model and the transient times differ; (ii) the damping of surge pressure is noticeably larger in comparison with the constant wave speed model; (iii) the surges are asymmetric with respect to the static head, while the pressure transient for the constant wave speed model was symmetric with respect to the static head. If there are evolution and subsequent absorption of the gas in the liquid along the pipeline, the initial upsurge caused by valve closure at the pumping station may be small but is very often followed by a delayed substantial pressure upsurge as shown in Figures 10 and 12 for pumping station C. This delayed substantial pressure upsurge

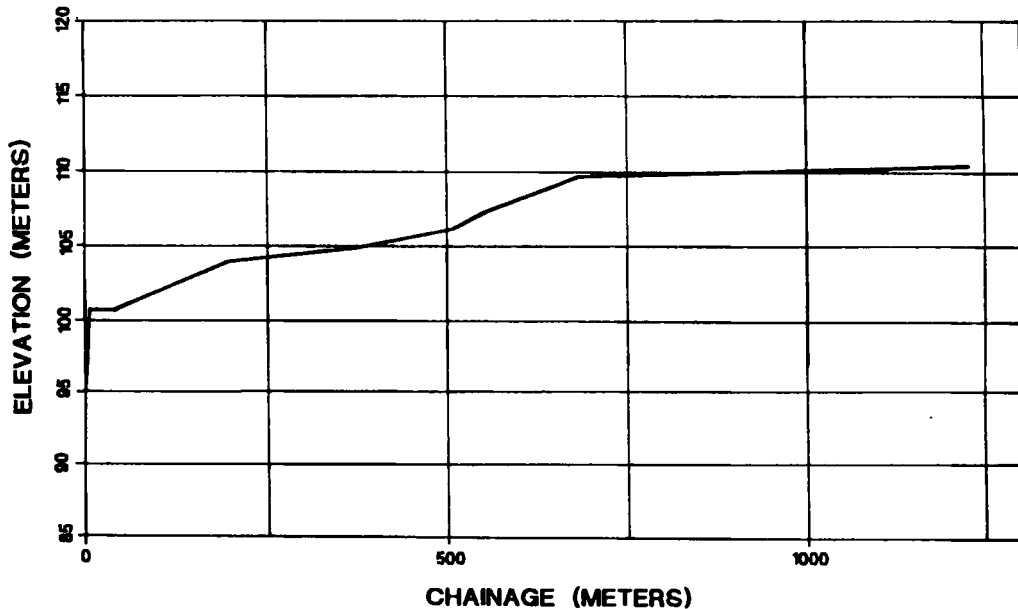


Figure 2. Pipeline contour for pumping station A

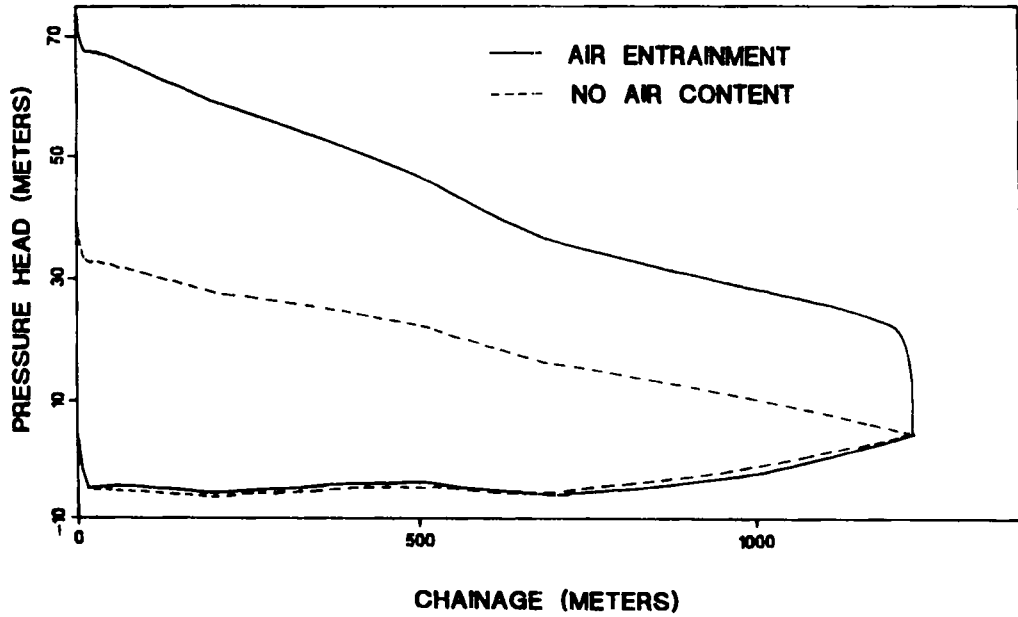


Figure 3. Maximum and minimum pressure head along pipeline A

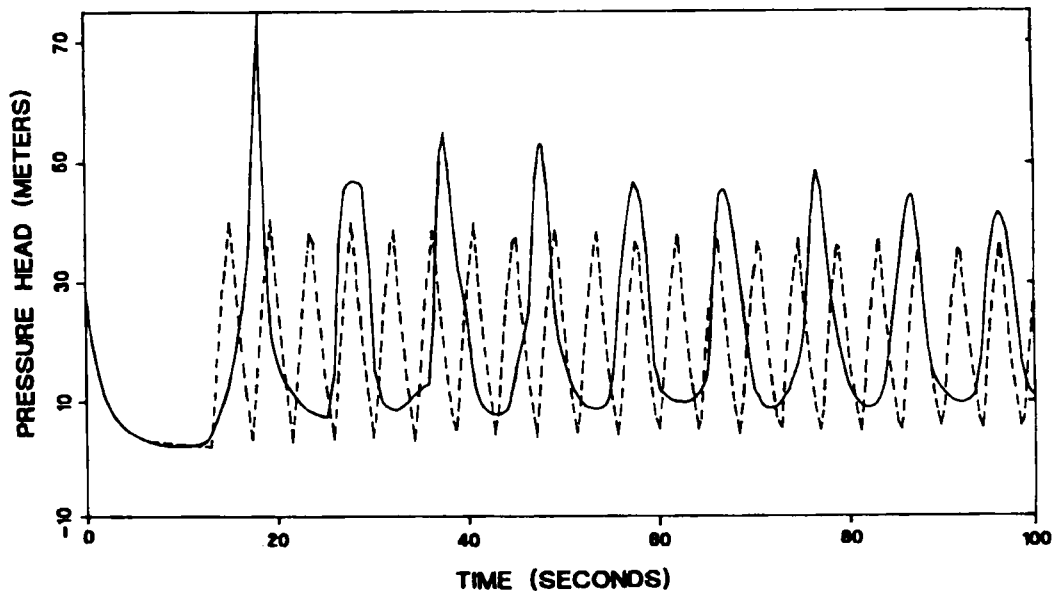


Figure 4. Pressure head downstream of pump A

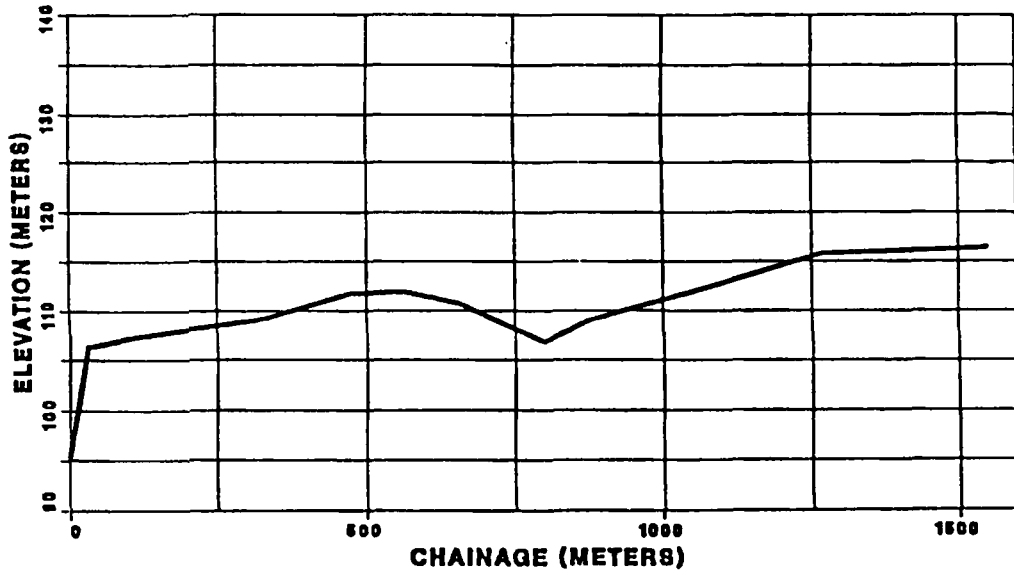


Figure 5. Pipeline contour for pumping station B

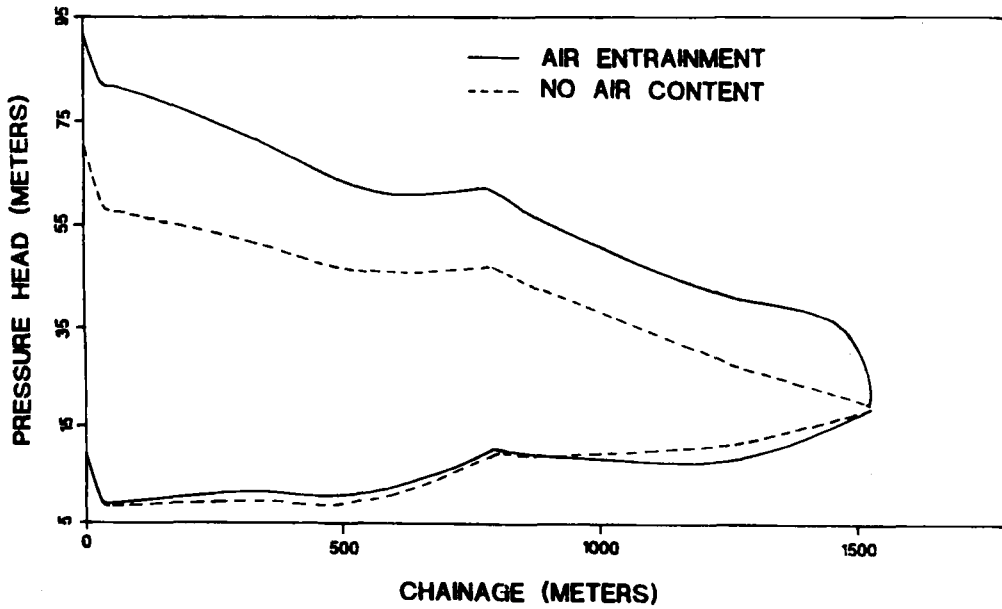


Figure 6. Maximum and minimum pressure head along pipeline B



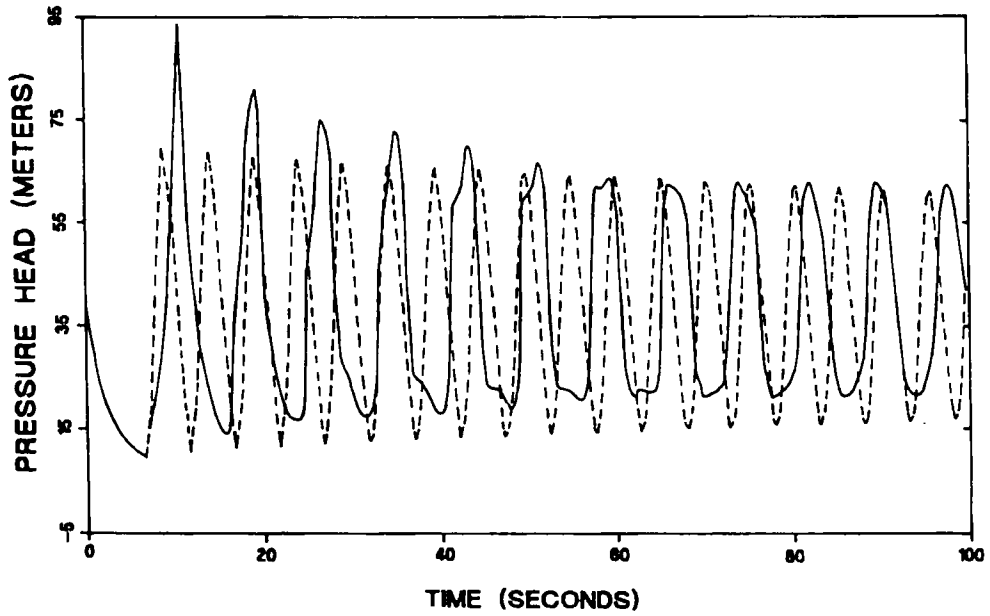


Figure 7. Pressure head downstream of pump B

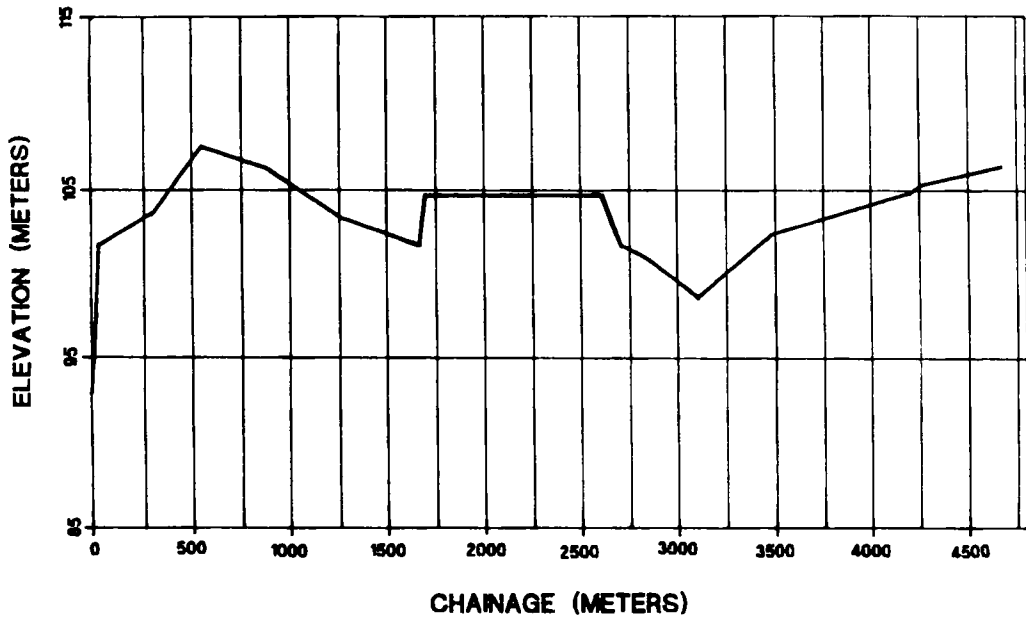


Figure 8. Pipeline contour for pumping station C

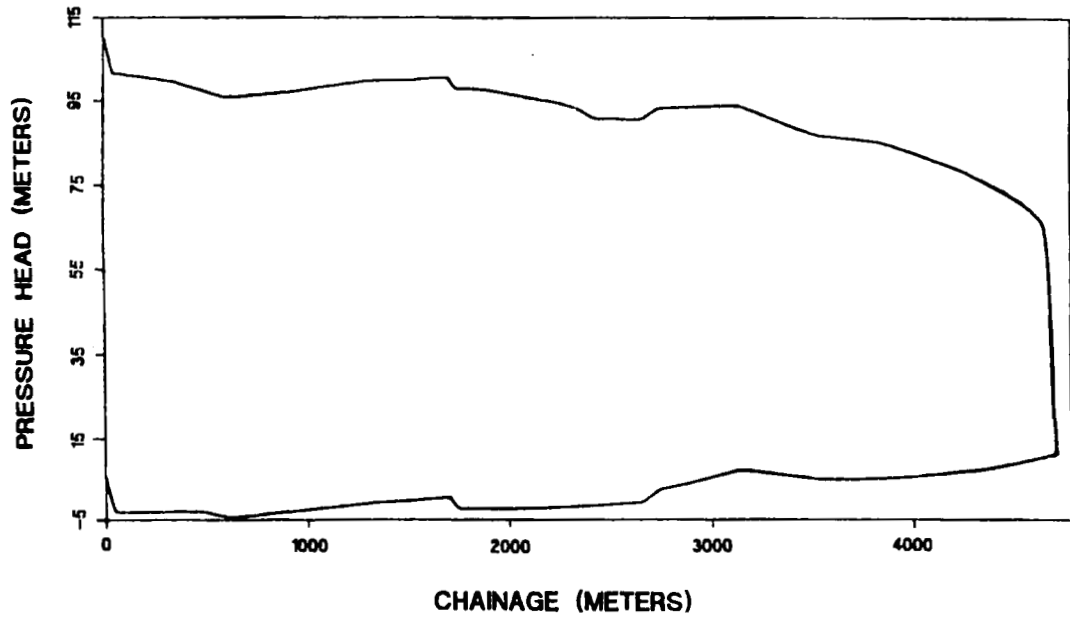


Figure 9. Maximum and minimum pressure head along pipeline C

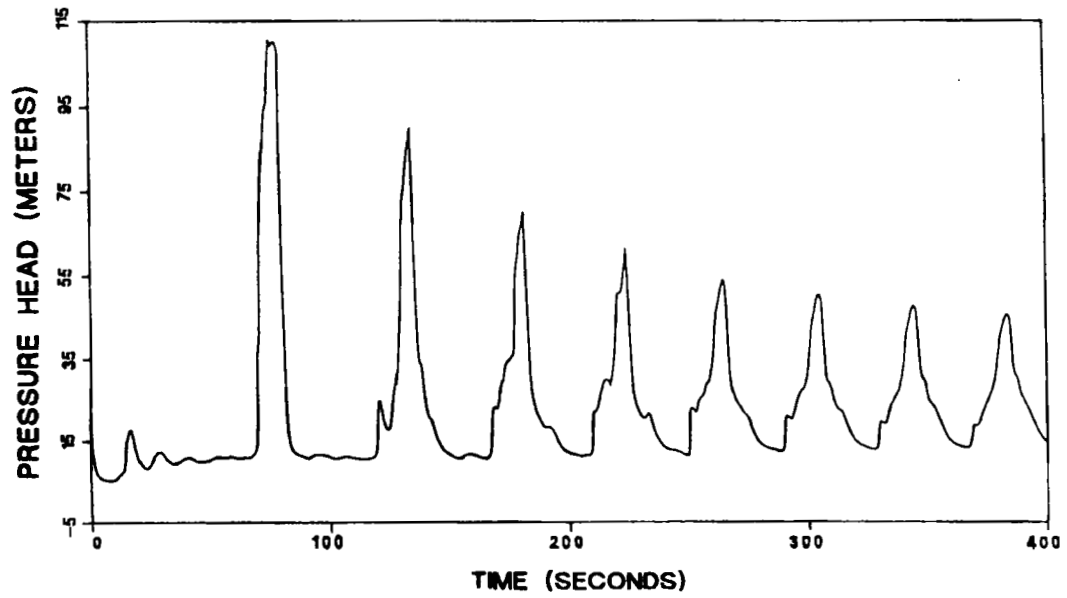


Figure 10. Pressure head downstream of pump C

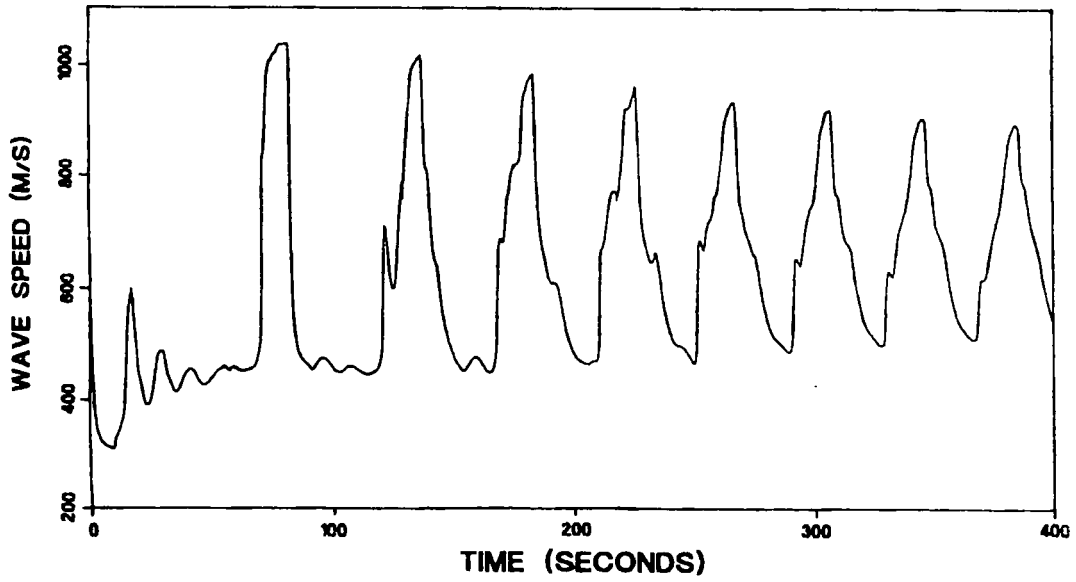


Figure 11. Wave speed downstream of pump C

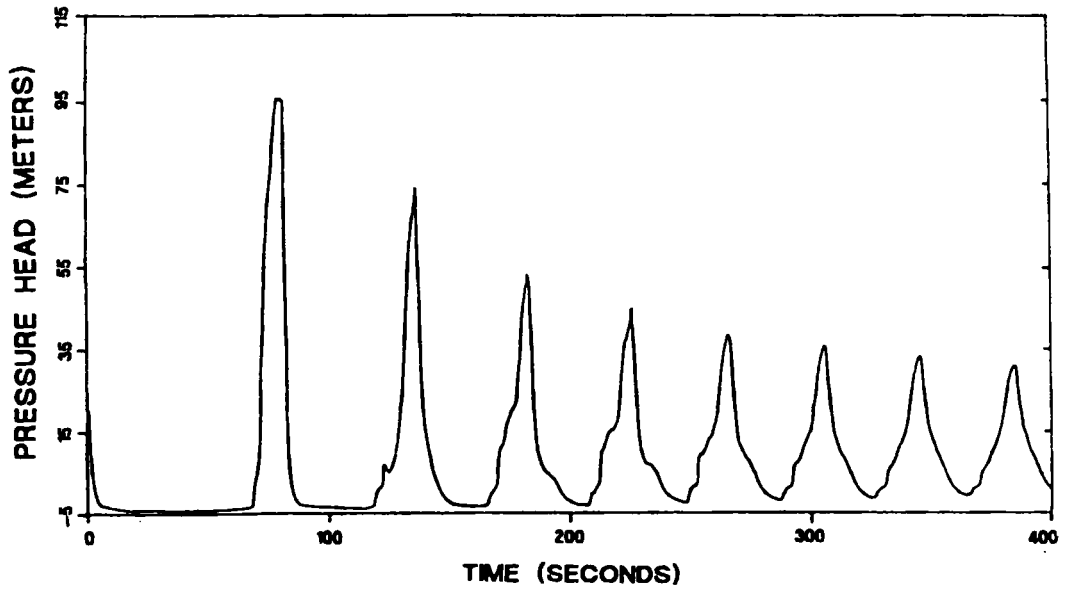


Figure 12. Pressure head at peak of elevation

due to gas release at the gas release head along the pipeline was also observed by Clarke.<sup>11</sup> The arrival of this substantial pressure upsurge at the pumping station generates a positive transient that travels upstream towards the reservoir. This positive transient raises the pressure along the pipeline and causes the free gas present in the flow to dissolve, so increasing the effective bulk modulus and thus the wave speed (as shown in Figure 11 for pumping station C). This positive pressure wave was then reflected off the downstream reservoir as a negative pressure wave. Owing to the higher pressure upstream of the reservoir, this negative pressure wave travels rapidly and arrests the large pressure upsurge at the pumping station. Hence the substantial pressure upsurge was present for a short duration. As the surge damping due to losses and the presence of air content sets in, the pressure downsurge along the pipeline usually does not subsequently fall below the gas release head and a regular oscillating pressure surge will then be observed. Hence the entrainment of free air and the release of gas at the gas release head reduce the local wave speed considerably and produce a complicated phenomenon of reflection of pressure waves off these 'cavities'. The lower local wave speed also increases the duration of the pressure downsurge as compared with the duration of the pressure upsurge.

The above characteristics were also observed experimentally by Whiteman and Pearsall,<sup>1,2</sup> Dawson and Fox<sup>12</sup> and Jonsson.<sup>13</sup> There are several reasons given in the literature for the increase in peak pressure during the pressure transient with air entrainment. Jonsson attributed the increase in peak pressure to the compression of 'an isolated air pocket' in the flow field after valve closure. Dawson and Fox attributed the increase in peak pressure to the 'cumulative effect of minor flow changes during the transient'. Through the numerous numerical experiments performed on the variable wave speed model, the authors observed that the greater peak pressure obtained for the variable wave speed model is due to the fact that the lower average wave speed delays the wave reflection at the reservoir and thus allows a more complex variation in pressure interaction to occur in the system, culminating in a peak at a specific transient interval. Falconer *et al.*<sup>14</sup> showed similarly through computer studies that it is possible for a low wave speed to increase the pressure peak even though a lower wave speed also implies a reduced change in pressure head for a given velocity change. Numerical experiments performed in this computer study also showed that the degree of amplification of the first pressure peak is dependent upon the rate of deceleration of the flow after pump trip. An increased pump inertia produces a slower rate of deceleration of the flow after pump trip and a smaller amplification of the first pressure peak as compared with the constant wave speed model.

Through the corresponding numerical experiments it is noted that friction and any devices put into the system have a damping effect on the pressure waves owing to the hysteresis in the energy cycle. However, it is also noted that the damping produced by losses alone is small and is independent of the local surge pressure encountered. This is evidenced in the constant wave speed model where the damping of the pressure transient is slow. For the variable wave speed model the damping of the pressure surge is fast. This is due to the fact that the gas content  $\varepsilon_i$  at a local point will increase as the lower-pressure wave is transmitted to that point during a downsurge and conversely  $\varepsilon_i$  will decrease as the higher-pressure wave is transmitted to the point during an upsurge of pressure. Hence there is an increase in local wave speed during upsurge and a decrease in local wave speed during downsurge. This also explains why the upsurge prediction in the variable wave speed model is higher than in the corresponding constant wave speed model and why the magnitude of the downsurge prediction is smaller in the variable wave speed model than in the constant wave speed model. Generally the numerical experiments show that the damping produced by the loss factor is much smaller than that produced by the gas content in the fluid during the pressure transient process. The precise physical cause of large surge damping in transient flow with gas content is still a subject of current research. However,

possible mechanisms have been suggested in the form of (i) direct damping due to the increased effective bulk viscosity of the fluid as a result of the presence of air bubbles,<sup>15</sup> (ii) losses due to slip between bubbles and water<sup>16</sup> and (iii) thermodynamic losses.<sup>17</sup> A mechanism due to indirect damping is explained by Pearsall<sup>9</sup> in his reflection hypotheses which states that when bubbly and unclear stretches of water alternate and interact, the partial wave reflections occurring at the interfaces break the periodic surge wave down. This explains the fast damping of the pressure transient in the variable wave speed model where air content is present.

## CONCLUSIONS

An improved numerical model has been developed to study the effects of air entrainment in the form of variable wave speed on the pressure transient in pumping installations. Variable free gas in the fluid and cavitation at vapour pressure were modelled. Numerical results showed that entrained, entrapped or released gases amplified the first pressure peak, increased surge damping and produced asymmetric pressure surges with respect to the static head. When air was entrained into the system, the pressure transient showed long periods of downsurge and short periods of upsurge. The upsurge was considerably amplified and the downsurge reduced in comparison with the gas-free constant wave speed case. The computed results showed good agreement with data available from other investigators of similar systems.<sup>3,13,14</sup>

## ACKNOWLEDGEMENT

The author gratefully acknowledges the kind assistance of the personnel from the Sewerage Department, Ministry of the Environment, Singapore for providing valuable information on pumping stations for this investigation. The support of a National University of Singapore research grant (RP890633) is also gratefully acknowledged.

## APPENDIX: NOMENCLATURE

<i>a</i>	wave speed
$A_1, A_2, A_3$	constants for pump $H-Q$ curve
$B_1, B_2, B_3$	constants for pump $T-Q$ curve
<i>c</i>	parameter describing pipe constraint condition
$C_1, C_2, C_3$	constants for pump $\eta-Q$ curve
<i>D</i>	mean diameter of pipe
<i>e</i>	local pipe wall thickness
<i>E</i>	modulus of elasticity
<i>f</i>	friction factor
<i>g</i>	gravitational acceleration
<i>H</i>	gauge piezometric pressure head
$H_g$	gas release pressure head (2.4 m water absolute)
<i>i</i>	node point at $x_i = (i - 1)\Delta x$
<i>I</i>	pump set moment of inertia including flywheel
<i>k</i>	time level at $t^k = \sum (\Delta t^k)$
<i>K</i>	bulk modulus of elasticity
<i>L</i>	length of pipe
$n_p$	number of pumps in pumping station
<i>N</i>	pump speed at node point <i>i</i> and time level <i>k</i> (rev min <sup>-1</sup> )

$N$	total number of node points along pipeline
$P$	pressure inside pipe
$Q$	fluid flow rate
$R$	$C^+$ -line intercept on $x$ -axis at $k$ th time level
$Re$	Reynolds number
$S$	$C^-$ -line intercept on $x$ -axis at $k$ th time level
$t$	time
$T$	pump torque
$V$	flow velocity
$x$	distance along pipeline
$z$	pipeline elevation w.r.t. pump intake level

### Greek letters

$\alpha$	pipeline inclination (positive downwards)
$\alpha_{ga}$	fraction of gas absorption
$\alpha_{gr}$	fraction of gas release
$\Delta t^k$	time step at time level $k$
$\Delta x$	node point distance along pipeline
$\epsilon$	fraction of air in liquid
$\epsilon_g$	fraction of dissolved gas in liquid
$\epsilon_o$	fraction of free gas in liquid at atmospheric pressure
$\eta$	pump efficiency
$\nu_g$	gas kinematic viscosity
$\nu_s$	sewage kinematic viscosity
$\rho$	density of fluid
$\tau$	valve closure function

### REFERENCES

1. K. J. Whiteman and I. S. Pearsall, 'Reflux valve and surge tests at Kingston pumping station', *BHRA/National Engineering Laboratory Joint Rep. 1*, 1959.
2. K. J. Whiteman and I. S. Pearsall, 'Reflux valve and surge tests at a station', *Fluid Handling*, **XIII**, 248–250 and 282–286 (1962).
3. R. J. Brown, 'Water-column separation at two pumping plants', *J. Basic Eng.*, **ASME**, 521–531 (1968).
4. G. A. Provoost, 'Investigation into cavitation in a prototype pipeline caused by waterhammer', *Proc. 2nd Int. Conf. on Pressure Surges*, Cranfield, September 1976, pp. 35–43.
5. E. B. Wylie, 'Free air in liquid transient flow', *Proc. 3rd Int. Conference on Pressure Surges*, Canterbury, March 1980, pp. 12–23.
6. J. A. Fox, 'Pressure transients in pipe networks—a computer solution', *Proc. 1st Int. Conf. on Pressure Surges*, Cranfield, September 1972, pp. 68–75.
7. J. A. Fox, *Hydraulic Analysis of Unsteady Flow In Pipe Network*, Macmillan, London, 1984.
8. T. S. Lee, 'Numerical computation of fluid pressure transients in pumping installations with air entrainment', *Int. j. numer. methods fluids*, **12**, 747–763 (1991).
9. I. S. Pearsall, 'The velocity of water hammer waves', *Proc. Inst. Mech. Eng.*, **180**, pt. 3E, 12–20 (1965–1966).
10. C. Kranenburg, 'Gas release during transient cavitation in pipes', *J. Hydraul. Div.*, **ASCE**, **100**, 1383–1398 (1974).
11. D. S. Clarke, 'Surge suppression—A warning', *Proc. Int. Conf. on the Hydraulics of Pumping Stations*, Manchester, September 1985, pp. 39–54.
12. P. A. Dawson and J. A. Fox, 'Surge analysis and suppression techniques for a water supply scheme—a case study', *Trans. Inst. Meas. Control*, **5**, (4) 134–142 (1983).
13. L. Jonsson, 'Maximum transient pressures in a conduit with check valve and air entrainment,' *Proc. Int. Conf. on the Hydraulics of Pumping Stations*, Manchester, September 1985, pp. 55–76.
14. R. H. Falconer, W. Banks and J. Ellis, 'Surge pressures at Riding Mill pumping station: actual values and theoretical predictions', *Proc. 4th Int. Conf. on Pressure Surges*, Bath, September 1983, pp. 427–445.

15. G. I. Taylor, 'The coefficients of viscosity for an incompressible liquid containing air bubbles', *Proc. R. Soc. A*, **226**, 34–39 (1954).
16. L. Van Wijngaarden, 'Some problems in the formulation of the equations for gas/liquid flows', in W. T. Koiter (ed.), *Theoretical and Applied Mechanics*, North-Holland, Amsterdam, 1976, pp. 365–372.
17. D. J. F. Ewing, 'Allowing for free air in waterhammer analysis', *Proc. 3rd Int. Conferon. Pressure Surges*, Canterbury, March 1980, pp. 80–91
18. C. Krandenburg, 'The effect of free gas on cavitation in pipelines induced by waterhammer', *Proc. 1st Int. Conf. on Pressure Surges*, Cranfield, September 1972.